# STRESS CONCENTRATION AROUND KNOTS IN LAMINATED BEAMS[1]

*R. C. Tang*

Professor of Wood Science
Department of Forestry, Auburn University, Auburn, AL 36849

(Received September 1981)

ABSTRACT

A formal elastic solution of the stresses and displacements occurring in a laminated beam, with an arbitrarily located elliptic or circular knot, subjected to static bending is presented. The solutions are obtained by using the theory of complex variables in plane elasticity. Numerical examples of the stress concentration are illustrated with graphs in which comparisons are made between the cases of sound knot, decayed knot, knothole, and wooden plug. The effects of size, shape, location, orientation, and material property of the knot on the stress concentrations are discussed.

*Keywords:* Knot effects, orientation of knots, laminated beams, St. Venant's Principle.

## INTRODUCTION

In recent years, laminated wood beams have been used in building constructions because they give many advantages over the other construction materials. However, there has been limited research on the strength-reducing effect of inhomogeneities and discontinuities associated with laminated wood beams. One of the most critical strength reducing defects in structural timbers is the knot and its associated grain deviation (Koch 1972). The effects of knots on the bending strength and stiffness of solid or laminated timbers depend upon the number, size, and position with respect to the neutral axis of the member, of the knots close to the critical section (Freas 1962; Siimes 1944; USDA 1974; Wangaard 1950). Although knowledge of stress distributions in a plate containing an elliptic, circular, and square hole under pure tension has been well documented (Lekhnitskii 1969; Savin 1961; Smith 1944; Tang 1968), information concerning the quantitative analyses of the effect of knots and knotholes on the stress concentrations in solid or laminated wood structural members is still very limited. However, using the finite element method, recent theoretical studies on the influence of knots on the tension behavior of wood revealed valuable information that could be useful in predicting tensile strength of wood members containing knots (Bartolomeo 1980; Goodman et al. 1980). In the case of beams subjected to static bending, the stress distribution in the vicinity of a knot or a knothole is very complicated (Price 1967). This is also evident from USDA's Wood Handbook (1974), which states "In beams having changes in cross-sectional dimension because of holes, bending stresses can be calculated at the hole by dividing the bending moment there by section modulus of the material remaining. Values of this bending stress are not useful in design because the change in cross section also causes shear stresses and stresses perpendicular to the beam neutral axis;

---

[1] The investigation reported in this paper (No. 9-82240) is in connection with a project of the Alabama Agricultural Experiment Station, Auburn University, and is published with the approval of the Director.

the combination of these stresses with the bending stress can cause failure at low load. It is not known how to compute these stresses . . . ." Admittedly, the variety of knots or knotholes and their grain deviations make the engineering analysis of stress concentration in a laminated beam under static bending very complex. However, for optimum design and effective utilization of laminated beams as a competitive structural material, it is important and necessary to understand the phenomena of stress concentration.

Using the technique of photoelasticity, the stress distribution in the vicinity of a knot and knothole located at the middle span of a solid wood beam was studied experimentally by Price (1967). He indicated that the strength-reducing factor is directly related to stress concentration due to the presence of knots or knotholes. Because of the complexity and diversity of grain deviation around the knot, no conclusive information was reported.

Although the flowgrain analogy technique has been applied in an attempt to model the grain deviation in the stress analysis of tension wood members containing a knot and showed promising results (Phillips et al. 1981), the wide variation of grain deviation around knots has limited such application to the idealized cases of symmetrically and smoothly deviated grains around knots of elliptic shape. However, Price (1967) suggested that better understanding of the effect of associated grain angle on the strength-reducing factors can be obtained mathematically by calculating the stress field around circular and elliptic knots in boards with various grain angles. With the excellent information on elastic properties of knotwood reported recently by Pugel (1980), such a mathematical model for stress concentration seems feasible.

Therefore, this investigation was aimed at developing an analytical model to predict the elastic stresses around knots, knotholes, and wooden plugs in simply supported laminated beams under a concentrated load. The results of the study are given herein for knots, knotholes, and wooden plugs of elliptic and circular shape. For simplicity of mathematical analyses, the grain deviations around the knot are neglected because their variations are so diverse and no definite pattern can be identified. However, to demonstrate indirectly the effect of grain deviation on the stress concentrations around the knot, different angles between the minor axis of an elliptic knot and the direction of wood grain were considered in the analysis. The effect of size, shape, location, and material properties of knots on the stress distributions are especially considered. Thus, the model presented does provide an indirect prediction of the effect of knots on the strength behavior of a laminated beam. However, because the investigation represents a pilot study on the effects of knots in laminated beams, the results are not reduced for design use. Additional work is needed in this regard. Hopefully, the analysis presented will provide a fundamental understanding of the influences of knots on the stress concentrations in structural beams and lead to the development of better and more accurate mathematical models.

## METHODS OF ANALYSIS

Consider a simply supported laminated beam, composed of two different orthotropic layers of arbitrary thickness, containing an elliptic knot in the tension zone of uniform shear span (Fig. 1a). To simplify the analysis, it is assumed that the knot is sufficiently remote from the reactions so the localized effects of these

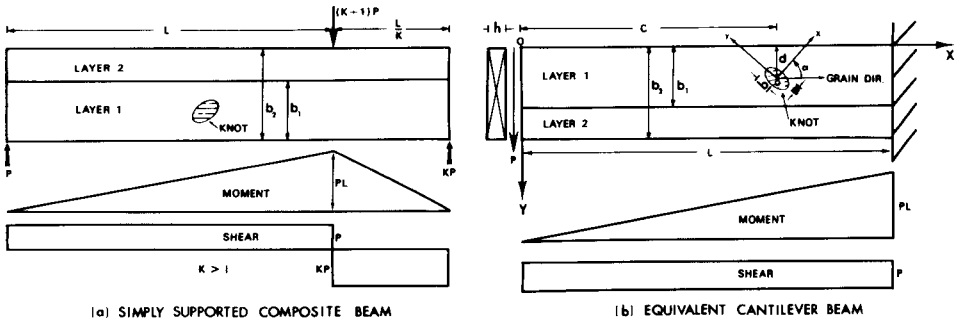


FIG. 1. Composite beam with an arbitrarily located knot.

forces do not extend near the knot. Furthermore, because the knot causes only localized redistributions of stress, the resulting perturbed stresses must attenuate, according to St. Venant's Principle, as distance from the knot increases. Based on the simple beam theory, by appropriately selecting the values of forces acting on the simply supported beam, the section containing a knot (length L) can be considered as a cantilever beam with a concentrated force (P) acting at the free end as shown in Fig. 1b. Therefore, the analysis of stress concentrations around a knot in this cantilever beam can be interpreted as the case of a simply supported beam. A similar approach was used in the analysis of buckling of webs with openings in I-beams (Uenoya and Redwood 1978).

Let h, L, and $b_2$ be the thickness, length, and depth of this cantilever beam, respectively. Assume that the beam is located in the XOY plane with X, Y axis along the upper rim and the free end, respectively, and the knot center is located at the point (c,d). Then, the components of stress of each layer in the absence of a knot can be expressed (Lekhnitskii 1969).

$$\sigma_X^{(1)} = \frac{6PE^{(1)}}{hS}(S_2 - 2S_1Y)X,$$

$$\sigma_X^{(2)} = \frac{E^{(2)}}{E^{(1)}}\sigma_X^{(1)},$$

$$\sigma_Y^{(1)} = \sigma_Y^{(2)} = 0,$$

$$\sigma_{XY}^{(1)} = \frac{6PE^{(1)}}{hS}(S_1Y_2^2 - S_2Y),$$

$$\sigma_{XY}^{(2)} = \frac{6PE^{(2)}}{hS}(S_2 - S_1b_2 - S_1Y)(b_2 - Y) \tag{1}$$

where $\sigma_X^{(j)}$, $\sigma_{XY}^{(j)}$, and $\sigma_Y^{(j)}$ (j = 1, 2) are the stress components of the jth layer in a beam without knot in the XOY system; $E^{(j)}$ is the Young's modulus in the X-direction of the jth layer; $b_j$ is the distance from the beam's upper rim to the lower edges of the jth layer; and S, $S_1$ and $S_2$ are defined as

$$S = b_1^4(E^{(1)})^2 + 2b_1(b_2 - b_1)(2b_2^2 - b_1b_2 + b_1^2)E^{(1)} + (b_2 - b_1)^4(E^{(2)})^2,$$
$$S_1 = b_1E^{(1)} + (b_2 - b_1)E^{(2)}, \quad S_2 = b_1^2E^{(1)} + (b_2^2 - b_1^2)E_1^{(2)}. \tag{2}$$

Since the center of the knot is at an arbitrary point (c, d), it is convenient

to use a new coordinate system xoy with the origin O at (c, d) in the XOY system. Due to the change of coordinates, the beam will behave anisotropically in the new xoy system. Then, the stresses relative to the xoy system can be expressed as

$$\begin{aligned}
\sigma_x^{(j)^o} &= A_1^{(j)}xy + A_2^{(j)}y^2 + A_3^{(j)}x + A_4^{(j)}y + A_5^{(j)},\\
\sigma_y^{(j)^o} &= B_1^{(j)}xy + B_2^{(j)}y^2 + B_3^{(j)}x + B_4^{(j)}y + B_5^{(j)},\\
\sigma_{xy}^{(j)^o} &= C_1^{(j)}xy + C_2^{(j)}y^2 + C_3^{(j)}x + C_4^{(j)}y + C_5^{(j)}, \qquad (j = 1, 2) \qquad (3)
\end{aligned}$$

where $\sigma_x^{(j)^o}$, $\sigma_y^{(j)^o}$, and $\sigma_{xy}^{(j)^o}$ are stress components of the jth layer in a beam without knot; and $A_j^{(j)}$, $B_k^{(j)}$, and $C_k^{(j)}$ ($k = 1, \ldots, 5$) are the arbitrary real constants related to the functions involving the end load (P), beam thickness (h), the elastic constants ($E^{(j)}$), the knot location (c, d), the angle ($\alpha$) between the ox axis and OX axis, and the S, $S_1$ and $S_2$, as given in Eq. 2. Such functions are not given herein because of their extreme length. Analogous to Likhnitskii's method (1969), the stresses ($\sigma_x^{(j)}$, $\sigma_y^{(j)}$, $\sigma_{xy}^{(j)}$) and the displacements ($u^{(j)}$, $v^{(j)}$) in a laminated beam with knots can be written as:

$$\begin{aligned}
\sigma_x^{(j)} &= \sigma_x^{(j)^o} + 2\,\mathrm{Re}[(\mu_1^{(j)})^2\phi_1^{(j)\prime}(z_1) + (\mu_2^{(j)})^2\phi_2^{(j)\prime}(z_2)],\\
\sigma_y^{(j)} &= \sigma_y^{(j)^o} + 2\,\mathrm{Re}[\phi_1^{(j)\prime}(z_1) + \phi_2^{(j)\prime}(z_2)],\\
\sigma_{xy}^{(j)} &= \sigma_{xy}^{(j)^o} + 2\,\mathrm{Re}[\mu_1^{(j)}\phi_1^{(j)\prime}(z_1) + \mu_2^{(j)}\phi_2^{(j)\prime}(z_2)], \qquad (j = 1, 2) \qquad (4)\\
u^{(j)} &= u^{(j)^o} + 2\,\mathrm{Re}[P_1^{(j)}\phi_1^{(j)}(z_1) + P_2^{(j)}\phi_2^{(j)}(z_2)] - \omega^{(j)^o}y + u_0^{(j)},\\
v^{(j)} &= v^{(j)^o} + 2\,\mathrm{Re}[q_1^{(j)}\phi_1^{(j)}(z_1) + q_2^{(j)}\phi_2^{(j)}(z_2)] + \omega^{(j)^o}x + v_0^{(j)}, \qquad (j = 1, 2) \qquad (5)
\end{aligned}$$

Here Re is the notation for the real part of the complex expression in the brackets; $\phi_1^{(j)\prime}$ and $\phi_2^{(j)\prime}$ are derivatives of analytic complex potentials $\phi_1^{(j)}$ and $\phi_2^{(j)}$ due to the presence of knot; $z_k$'s are complex variables defined as $z_k = x + \mu_k y$ ($k = 1, 2$); $u^{(j)^o}$ and $v^{(j)^o}$ are the displacements in the beam without knots; $\omega^{(j)^o}$, $u_0^{(j)}$ and $v_0^{(j)}$ are rigid body displacements of the beam; and

$$P_k^{(j)} = a_{11}^{(j)}(\mu_k^{(j)})^2 + a_{12}^{(j)} - a_{16}^{(j)}\mu_k^{(j)}; \quad q_k^{(j)} = a_{12}^{(j)}\mu_k^{(j)} + \frac{a_{22}^{(j)}}{\mu_k^{(j)}} - a_{26}^{(j)} \qquad (6)$$

where $\mu_k^{(j)}$'s are the complex parameters of beam property related to the roots of the algebraic equation:

$$a_{11}^{(j)}\mu^4 - 2a_{16}^{(j)}\mu^3 + (2a_{12}^{(j)} + a_{66}^{(j)})\mu^2 - 2a_{26}^{(j)}\mu + a_{22}^{(j)} = 0, \qquad (7)$$

where $a_{11}^{(j)}$, $a_{22}^{(j)}$, $a_{12}^{(j)}$, $a_{66}^{(j)}$, $a_{16}^{(j)}$, and $a_{26}^{(j)}$ are the elastic compliances of the jth layer.

By carefully examining the stress components for a beam in the absence of knots as expressed in Eq. 3, the general stress function for a beam when a knot is present, can be expressed as:

$$\begin{aligned}
F^{(j)} = {} & D_0^{(j)}x^4 + D_1^{(j)}x^3y + D_2^{(j)}x^2y^2 + D_3^{(j)}xy^3 + D_4^{(j)}y^4 + D_5^{(j)}x^3\\
& + D_6^{(j)}x^2y + D_7^{(j)}xy^2 + D_8^{(j)}y^3 + D_9^{(j)}x^2 + D_{10}^{(j)}xy + D_{11}^{(j)}y^2 \qquad (8)
\end{aligned}$$

where $D_m^{(j)}$'s ($m = 0, 1, 2, \ldots, 11$) are unknown constants to be determined from the boundary conditions. It should be noted here that $D_m^{(j)}$'s are varied with the location, shape, size, and material properties of the knot.

Let $F^{(j)}$ be the stress function for the jth layer in a beam with a knot; then, the boundary conditions for $\phi_1^{(j)}$ and $\phi_2^{(j)}$ in Eqs. 4–5 can be written as

$$\begin{aligned}
2\,\mathrm{Re}[\phi_1^{(j)}(z_1) + \phi_2^{(j)}(z_2)] &= f_1^{(j)},\\
2\,\mathrm{Re}[\mu_1^{(j)}\phi_1^{(j)}(z_1) + \mu_2^{(j)}\phi_2^{(j)}(z_2)] &= f_2^{(j)}\\
2\,\mathrm{Re}[P_1^{(j)}\phi_1^{(j)}(z_1) + P_2^{(j)}\phi_2^{(j)}(z_2)] &= u^{(j)\prime} - u^{(j)\prime\prime} + \omega^{(j)\prime\prime}y - u_0^{(j)},\\
2\,\mathrm{Re}[q_1^{(j)}\phi_1^{(j)}(z_1) + q_2^{(j)}\phi_2^{(j)}(z_2)] &= v^{(j)\prime} - v^{(j)\prime\prime} - \omega^{(j)\prime\prime}x - v_0^{(j)}, \quad (j = 1, 2) \quad (9)
\end{aligned}$$

where $u^{(j)\prime}$ and $v^{(j)\prime}$ are the displacements of the knot; and $f_1^{(j)}$ and $f_2^{(j)}$ are defined as:

$$\begin{aligned}
f_1^{(j)} &= (D_3^{(j)} - H_1^{(j)})y^3 + (2D_2^{(j)} - H_2^{(j)})y^2x + (3D_1^{(j)} - H_3^{(j)})x^2y + 4D_0^{(j)}x^3\\
&\quad + (D_7^{(j)} - H_4^{(j)})y^2 + (2D_6^{(j)} - H_5^{(j)})xy + (3D_5^{(j)} - H_6^{(j)})x^2\\
&\quad + (D_{10}^{(j)} - H_7^{(j)})y + (2D_9^{(j)} - H_8^{(j)})x + H_9^{(j)},\\
f_2^{(j)} &= (4D_4^{(j)} + G_1^{(j)})y^3 + (3D_3^{(j)} + G_2^{(j)})y^2x + (2D_2^{(j)} + G_3^{(j)})x^2y\\
&\quad + D_1^{(j)}x^3 + (3D_8^{(j)} + G_4^{(j)})y^2 + (2D_7^{(j)} + G_5^{(j)})xy + (D_6^{(j)} + G_6^{(j)})x^2\\
&\quad + (2D_{11}^{(j)} + G_7^{(j)})y + (D_{10}^{(j)} + G_8^{(j)})x + G_9^{(j)}, \quad (j = 1, 2) \quad (10)
\end{aligned}$$

where $G_n^{(j)}$'s and $H_n^{(j)}$'s (n = 1, 2, . . . , 9) are designated as the real constants which are related to the known constants $A_k^{(j)}$, $B_k^{(j)}$, $C_k^{(j)}$ given in Eq. 3.

In order to calculate the stresses at the edge of an elliptic knot, it is convenient to express the analytic complex function $\phi_k^{(j)}(z_k)$ in an elliptic coordinate. By applying the mapping technique for complex variables $Z_k$, we have

$$\begin{aligned}
\phi_k^{(j)}(z_k) = M_k^{(j)} + \frac{1}{8(\mu_1^{(j)} - \mu_2^{(j)})}\Big\{&\Big[3ib^3(4D_4^{(j)} + G_1^{(j)} - \mu_\lambda^{(j)}(D_3^{(j)} - H_1^{(j)}))\\
&+ ab^2(3D_3^{(j)} + G_2^{(j)} - \mu_\lambda^{(j)}(2D_2^{(j)} - H_2^{(j)}))\\
&+ ia^2b(2D_2^{(j)} + G_3^{(j)} - \mu_\lambda^{(j)}(3D_1^{(j)} - H_3^{(j)}))\\
&+ 3a^3(D_1^{(j)} - 4\mu_\lambda^{(j)}D_0^{(j)})\\
&+ 4ib(2D_{11}^{(j)} + G_7^{(j)} - \mu_\lambda^{(j)}(D_{10}^{(j)} - H_7^{(j)}))\\
&+ 4a(D_{10}^{(j)} + G_8^{(j)} - \mu_\lambda^{(j)}(2D_9^{(j)} - H_8^{(j)}))\Big]\frac{1}{\zeta_k}\\
&+ \Big[2ib(2D_7^{(j)} + G_5^{(j)} - \mu_\lambda^{(j)}(2D_6^{(j)} - H_5^{(j)}))\\
&\quad - 2b^2(3D_8^{(j)} + G_4^{(j)} - \mu_\lambda^{(j)}(D_7^{(j)} - H_4^{(j)}))\\
&\quad + 2a^2(D_6^{(j)} + G_6^{(j)} - \mu_\lambda^{(j)}(2D_5^{(j)} - H_6^{(j)}))\Big]\frac{1}{\zeta_k^2}\\
&+ \Big[a^3(D_1^{(j)} - 4\mu_\lambda^{(j)}D_0^{(j)})\\
&\quad + ia^2b(2D_2^{(j)} + G_3^{(j)} - \mu_\lambda^{(j)}(3D_1^{(j)} - H_3^{(j)}))\\
&\quad - ab^2(3D_3^{(j)} + G_2^{(j)} - \mu_\lambda^{(j)}(2D_2^{(j)} - H_2^{(j)}))\\
&\quad - ib^3(4D_4^{(j)} + G_1^{(j)} - \mu_\lambda^{(j)}(D_3^{(j)} - H_1^{(j)}))\Big]\frac{1}{\zeta_k^3}
\end{aligned}$$

$$+ ab^2(3D_8^{(j)} + G_4^{(j)} - \mu_\lambda^{(j)}(D_7^{(j)} - H_4^{(j)}))$$
$$+ 2a^2(D_6^{(j)} + G_6^{(j)} - \mu_\lambda^{(j)}(D_3^{(j)} - H_1^{(j)}))\Big\},$$
$$(k, \lambda = 1, 2 \quad \text{and} \quad k \neq \lambda) \qquad (11)$$

where $$z_k = x + \mu_k y = \frac{a - i\mu_k b}{2}\zeta_k + \frac{a + i\mu_k b}{2}\frac{1}{\zeta_k}, \qquad (k = 1, 2)$$

and $x = a \cos \theta$, $y = b \sin \theta$, and a, b are the semi-axes of the elliptic knot.

It was found in Eqs. 9–11 that there are thirty-four unknown constants. They are $D_m^{(j)}$ ($m = 0, 1, \ldots, 11$), $M_1^{(j)}$, $M_2^{(j)}$, $u_0^{(j)}$, $v_0^{(j)}$, and $(\omega^{(j)'} - \omega^{(j)''})$, the rotation of the knot with respect to the beam. To determine these unknown constants, one must substitute the elastic constants of each layer and knot into Eqs. 9–11. Doing so, a set of sixteen lengthy and complicated equations can be obtained. Because of the involvement of complex variables, the substitution of $-i$ for i in these equations will yield sixteen more equations. These thirty-two equations are not given herein because of their extreme length. In order to solve this problem, two more equations are needed. They can be obtained from the stress-strain relation in the knot with respect to the jth layer of the beam. That is

$$6a'_{11}D_4^{(j)} - 3a'_{16}D_3^{(j)} + (2a'_{12} + a'_{66})D_2^{(j)} - 3a'_{26}D_1^{(j)} + 6a'_{22}D_0^{(j)} = 0, \quad (j = 1, 2)$$

where $a'_{11}$, $a'_{12}$, $a'_{22}$, $a'_{16}$, $a'_{26}$ and $a'_{66}$ are elastic compliances of the knot.

Let $\sigma_\eta^{(j)}$ be the stress normal to the knot; $\sigma_\xi^{(j)}$ the stress tangential to the knot, and $\sigma_{\eta\xi}^{(j)}$ the shearing stress, then, from Eq. 4, we have

$$\sigma_\eta^{(j)} = 2(a^2\sin^2\theta + b^2\cos^2\theta)^{-1}\mathrm{Re}[(a \sin \theta - \mu_1^{(j)}b \cos \theta)^2\phi_1^{(j)'}(z_1)$$
$$+ (a \sin \theta - \mu_2^{(j)}b \cos \theta)^2\phi_2^{(j)'}(z_2)] + \sigma_\eta^{(j)''},$$
$$\sigma_\xi^{(j)} = -2(a^2\sin^2\theta + b^2\cos^2\theta)^{-1}\mathrm{Re}[(b \cos \theta + \mu_1^{(j)}a \sin \theta)^2\phi_1^{(j)'}(z_1)$$
$$+ (b \cos \theta + \mu_2^{(j)}a \sin \theta)^2\phi_2^{(j)'}(z_2)] + \sigma_\xi^{(j)''},$$
$$\sigma_{\eta\xi}^{(j)} = 2(a^2\sin^2\theta + b^2\cos^2\theta)^{-1}\mathrm{Re}[(a \sin \theta - \mu_1^{(j)}b \cos \theta)$$
$$\cdot(b \cos \theta + \mu_1^{(j)}a \sin \theta)\phi_1^{(j)'}(z_1)$$
$$+ (a \sin \theta - \mu_2^{(j)}b \cos \theta)(b \cos \theta + \mu_2^{(j)}a \sin \theta)\phi_2^{(j)'}(z_2)] + \sigma_\xi^{(j)''} \qquad (12)$$

where $\sigma_\eta^{(j)''}$, $\sigma_\xi^{(j)''}$, $\sigma_{\eta\xi}^{(j)''}$ are stresses in the elliptical coordinates obtained from the transformation of stress components in Eq. 3. Then from Eq. 12, the stresses around the knot are ready to be determined.

## NUMERICAL CALCULATIONS

Because the experimental findings indicate that the knot reduces the strength of a wood beam considerably if it is located in the tension zone, therefore, in this investigation, the numerical analyses were focused on the cases of knots located in layer 1. To illustrate the effect of size, shape, and position of knot on the stress distribution around the knot, laminated beams with the following parameters are considered in the numerical calculation:

| | |
|---|---|
| Dimension of beam: | 2 in. (thickness, h) × 10 in. (depth, $b_2$) × 192 in. (length, L) |
| Depth of layer: | layer (1)/layer (2) = 5 in./5 in. |
| Position of knot: | at high shear-moment ratio (9.60/L) section<br>(c, d) = (20 in., 2 in.) and (20 in., 3 in.)<br>at low shear-moment ratio (1.1163/L) section<br>(c, d) = (172 in., 2 in.) and (172 in., 3 in.) |
| Orientation of knot: | 0°, vertical elliptic knot,<br>45°, inclined elliptic knot,<br>90°, horizontal elliptic knot |
| Size of knot: | ratio of semi-axis in the knot, a/b =<br>0.5 in./1 in. (large elliptic knot),<br>0.25 in./0.5 in. (small elliptic knot),<br>1 in./1 in. (large circular knot),<br>0.5 in./0.5 in. (small circular knot) |
| Material of layer: | layer 1—Douglas-fir and layer 2—Southern pine |
| Material of knot: | 1. sound knot<br>2. decayed knot<br>3. knothole<br>4. replaced by a wooden plug |

Using the above data with the elastic compliances given in Table 1, the stress distributions along the edge of knot were calculated from Eq. 12. The results for cases of knots located at high bending moment section (shear-moment ratio: 1.116/L) are graphically illustrated in Figs. 2–10. In all figures, the values of stress/load, generally considered to be the index of stress concentration, are plotted vs. the polar angles at different contour points around the knot. It should be noted here that the magnitude of normal stress ($\sigma_x$) along grain direction at the beam upper rim 20 in. and 172 in. away from the free end, in the absence of knot, are 0.559 P/in.$^2$ and 4.804 P/in.$^2$, respectively. This information can be used as a reference for the comparison of stress concentrations with the cases when the knot is present at that section.

## RESULTS AND DISCUSSION

### *Effects of material properties of knot*

Typical computer plots of the variation of the stress concentration factor (stress/load) along the edge of vertical knots, showing the effect of knot properties, are

TABLE 1. *Elastic compliances of beam and knot with reference to XOY system (unit: $10^{-6}$/psi).*

| Material | $a_{11}$ | $a_{22}$ | $a_{12}$ | $a_{66}$ | $a_{16}$ | $a_{26}$ |
|---|---|---|---|---|---|---|
| *Douglas-fir (8) | 0.5495 | 10.9890 | −0.2468 | 7.0423 | 0 | 0 |
| *Southern pine (4) | 0.6579 | 15.3139 | −0.3063 | 10.7875 | 0 | 0 |
| Sound knot (8) | 22.3717 | 17.7305 | −10.4444 | 30.3030 | 0 | 0 |
| Decayed knot | 10 times higher than those of sound knot | | | | | |
| Knothole | ∞ | ∞ | ∞ | ∞ | ∞ | ∞ |
| Wooden plug (Douglas-fir) | 10.9890 | 0.5495 | −0.2468 | 7.0423 | 0 | 0 |

* For the case $\alpha = 0°$, i.e. grain direction is parallel to the beam axis.

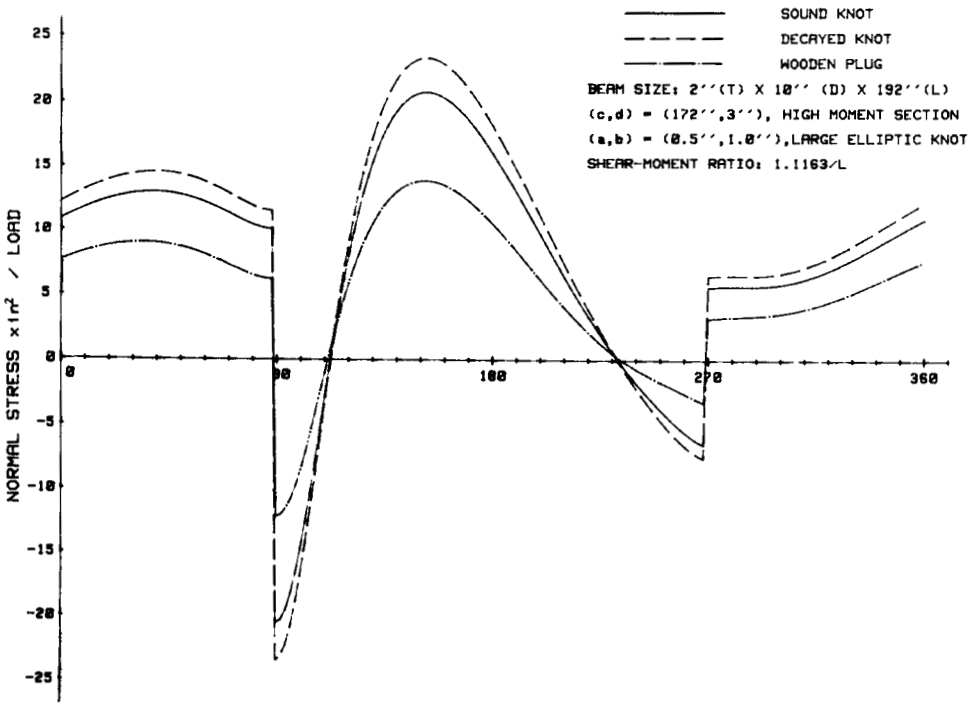


FIG. 2. Distribution of normal stress around a vertical knot ($\alpha = 0°$).

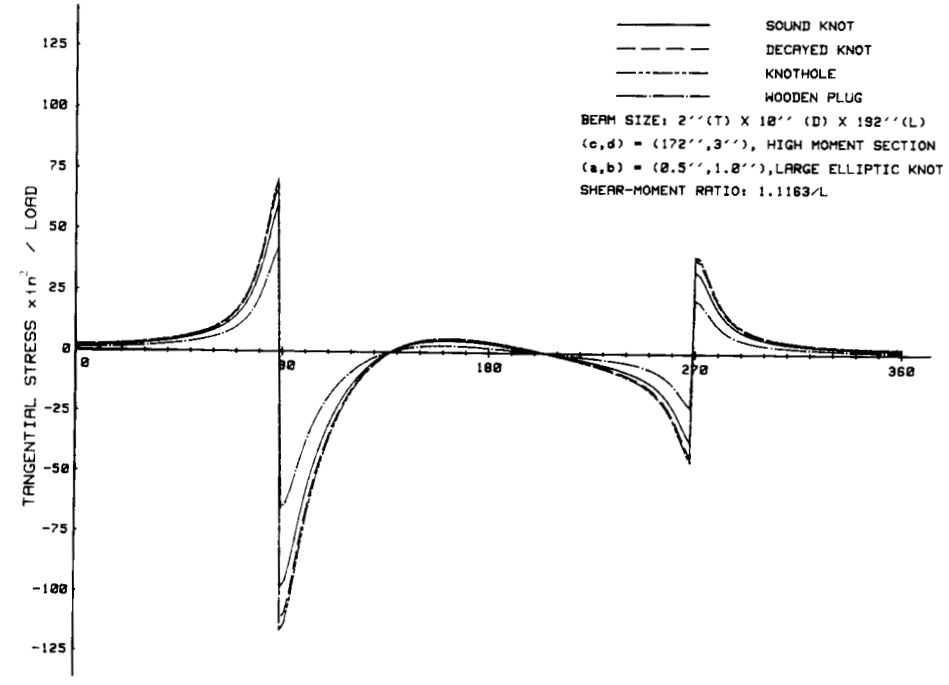


FIG. 3. Distribution of tangential stress around a vertical knot ($\alpha = 0°$).

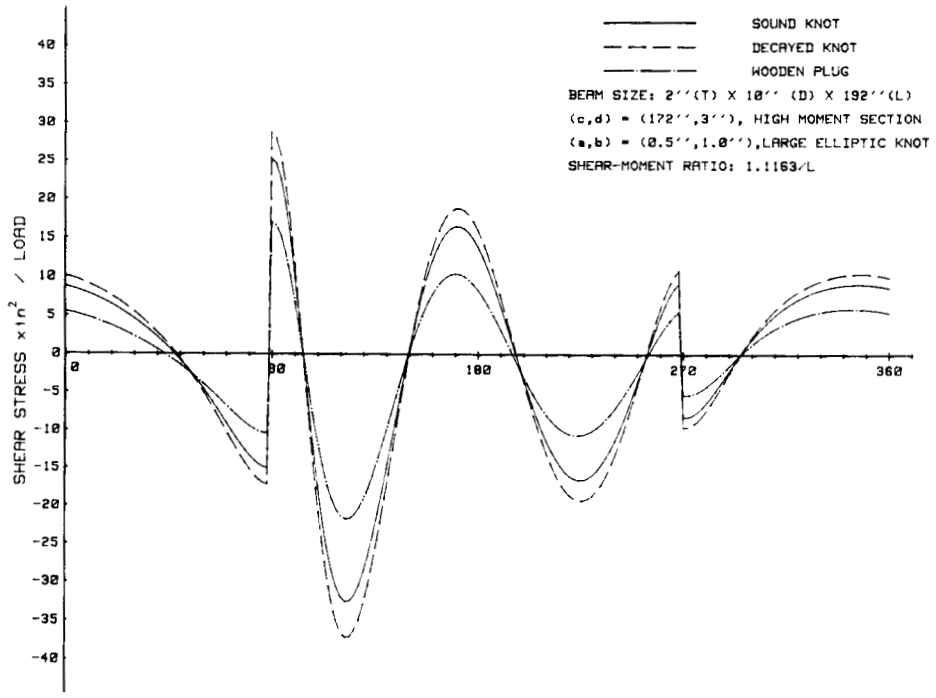


FIG. 4. Distribution of shear stress around a vertical knot ($\alpha = 0°$).

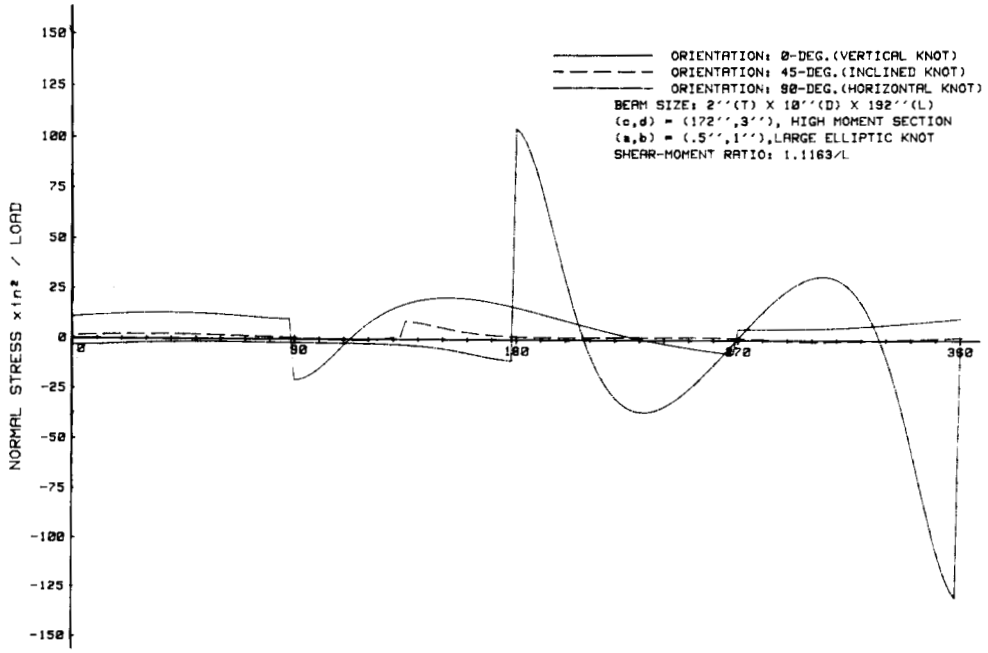


FIG. 5. Distribution of normal stress around a sound knot.

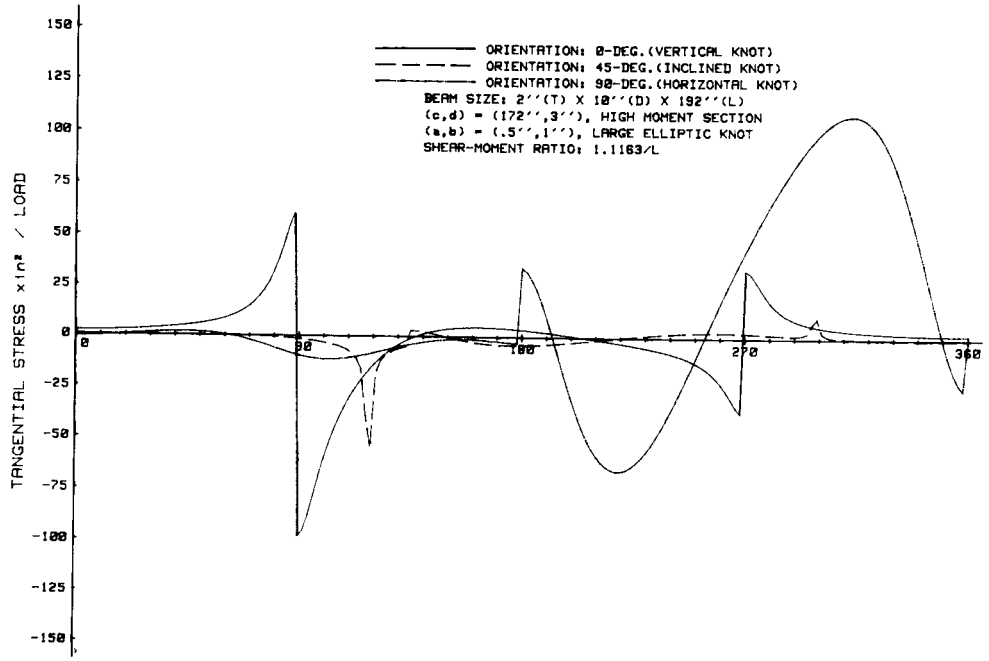


FIG. 6. Distribution of tangential stress around a sound knot.

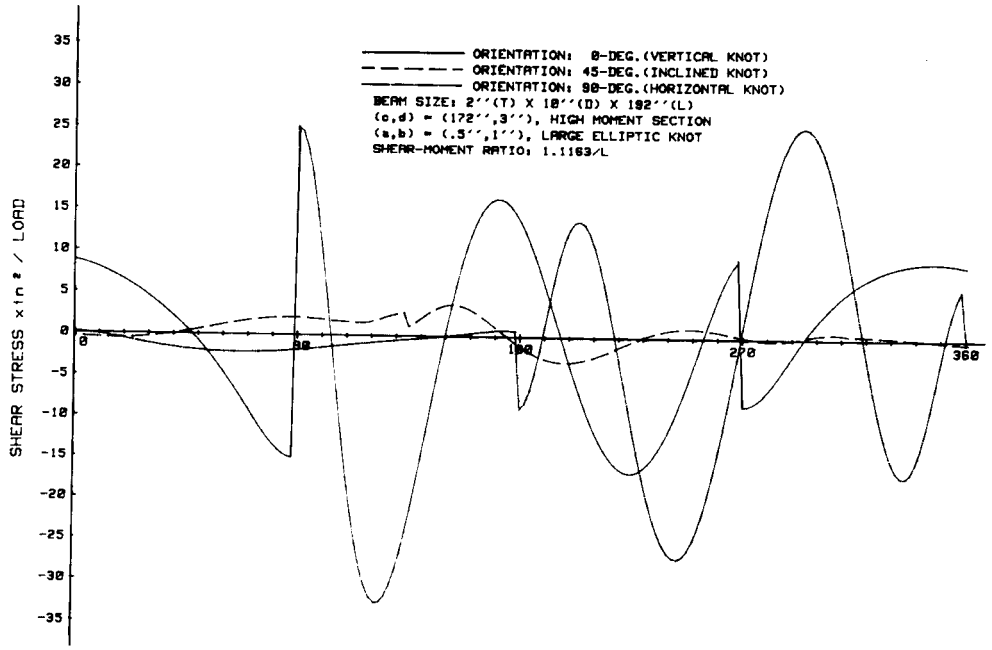


FIG. 7. Distribution of shear stress around a sound knot.

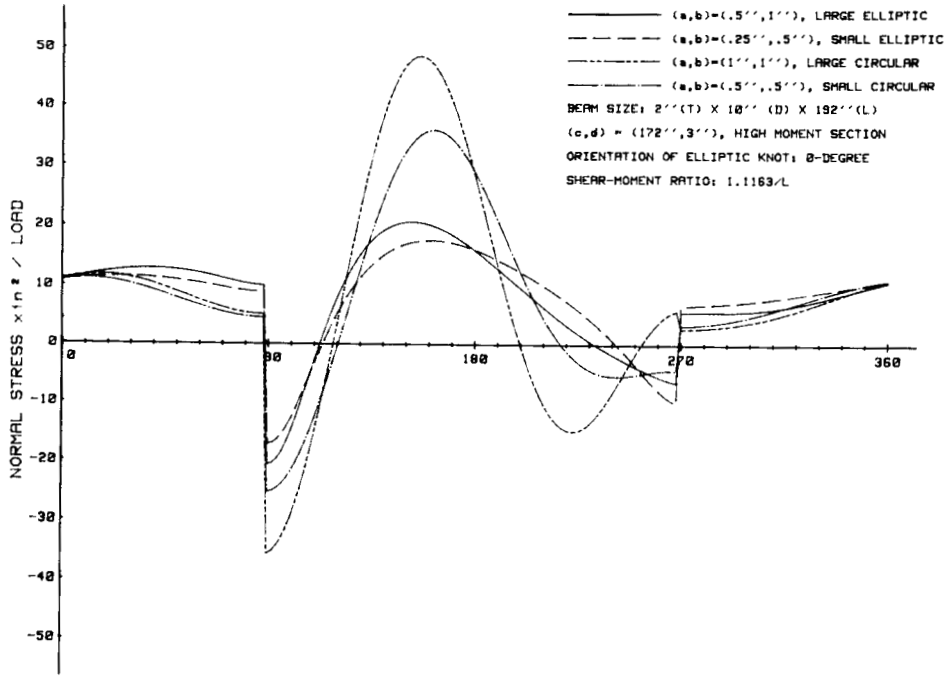


FIG. 8. Distribution of normal stress around a sound knot.

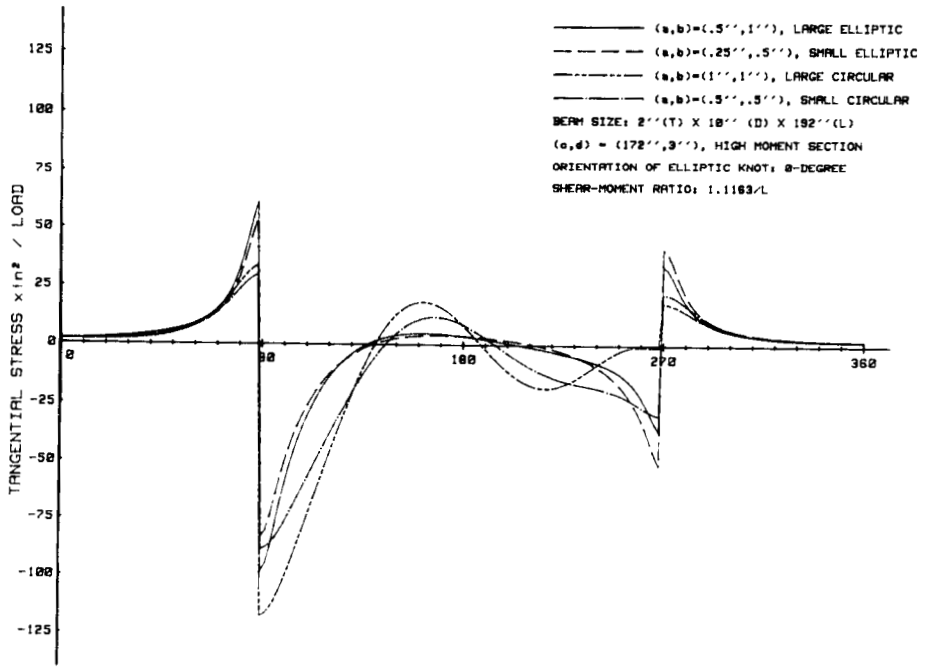


FIG. 9. Distribution of tangential stress around a sound knot.

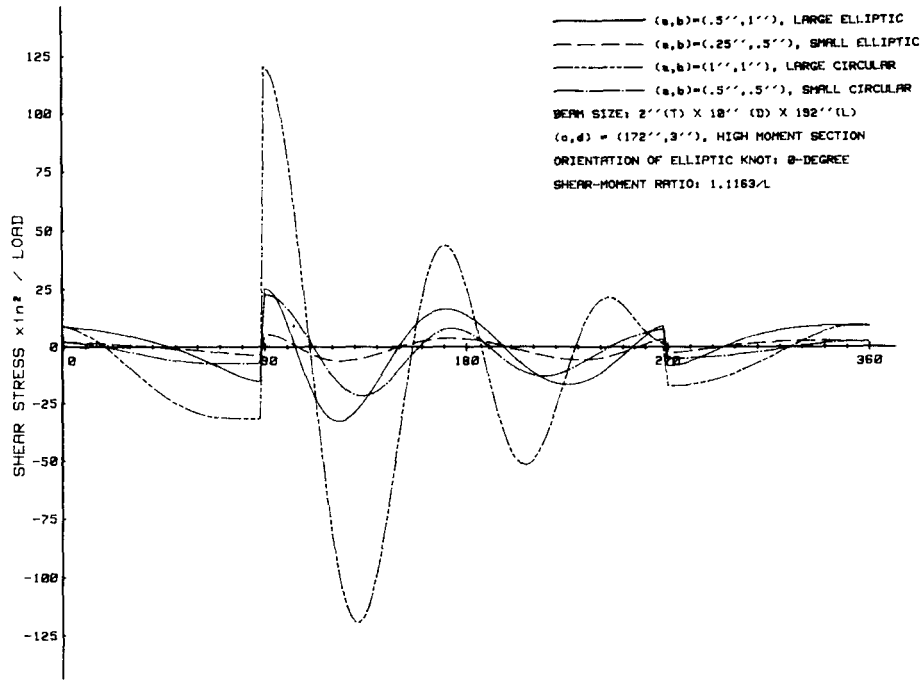


FIG. 10. Distribution of shear stress around a sound knot.

given in Figs. 2–4. Regardless of knot size and material properties, the general patterns of stress distribution are somewhat alike within each orientation group. The decay or missing of knot materials will significantly increase the stress concentration. However, the replacement of a knot with a wooden plug, if it is tightly bonded to the knothole, will reduce the stress concentration approximately 27% in a circular knot and 35% in an elliptic knot regardless of its size.

In the case of vertical elliptic knots, regardless of its size and material properties, the positive maximum shear stress will occur around the vicinity of the vertical knot apex near the beam's rim. The negative maximums of tangential and normal stress will be developed at the same area. This suggests that failure of a simply supported laminated beam containing a vertical elliptic knot in the tension zone, and subjected to a concentrated load, could be initiated around the vicinity of its vertical apex near the beam's rim. Furthermore, the combined effects of these stresses could trigger the beam failure at a very low load. These findings enhance the statement made by USDA's Forest Products Laboratory (1974) regarding beam failure at low load being caused by the combination of shear stresses and stress perpendicular to the beam neutral axis with the bending stresses. In the case of horizontal elliptic knots, the beam failure may initiate in the neighborhood between the horizontal and vertical apex at the higher moment side, and it varies with the knot size and material properties.

### *Effects of knot shape*

Influences of knot shape on the stress concentrations are somewhat mixed. Regardless of knot size and material type, both positive and negative maximum

of normal stresses developed in a circular knot are much higher than those of a vertical elliptic knot (Fig. 8). However, the situation is reversed when compared with a horizontal elliptic knot. The positive maximum of tangential stress in a circular knot is much lower than in those of elliptic shape regardless of size and orientation (Fig. 9). No significant difference was found between their negative maximums except those horizontal ones, which are considerably lower. Both positive and negative maximum of shear stress developed in a circular knot are significantly higher than in those of elliptic shape regardless of its size, orientation, and material (Fig. 10). Obviously, such variations are probably attributed to the combined effects of knot curvature and dimension. This is understandable because in this study the dimension of circular knots is twofold larger than the elliptic ones. However, the occurrences of stress concentrations in a circular knot, regardless of its material and size, are very much similar to those of vertical elliptic knots. Therefore, it can be anticipated that their failure mode will be somewhat alike.

### *Effects of the orientation of knots*

The maximum normal stress occurring in a horizontal elliptic knot, regardless of its size, is considerably higher than that in a vertical knot. When the elliptic knot is inclined 45° away from grain direction, regardless of its size and material property, all stress concentrations are pronouncedly reduced. In contrast, substantial increases in positive and negative normal stresses and positive tangential stress around the knot are found when the knot is 0° and 90° oriented. However, reduction in both positive and negative shear stresses and negative tangential stress due to the 45° orientation is visible but not significant. On the basis of these findings, one may expect that, if the wood grain is deviated gradually and smoothly around a knot, the normal stresses will be relatively increased and the tangential stresses will be relatively decreased while the change in shear stresses will be very small.

### *Effects of knot size*

It was found that, regardless of knot shape, decrease in knot dimension does not alter the pattern of stress concentrations. However, as shown in Figs. 8–10, a 50% decrease in knot dimension will significantly reduce all the stress concentrations. The shear stresses, considered to be critical to the initiation of beam failure when knots are present, are substantially reduced. These results may provide useful information to wood structural engineers in the design and safety of wood structures when the shear is critical.

### *Effects of knot location*

The stress concentrations in a knot, regardless of its shape and size, located at the high shear-moment ratio section on tension zone (low moment area) will be approximately 88% less than those located at low shear-moment ratio section (high moment area). Substantial decrease in the stress concentrations was found in the case when the knot is located in the compression zone of a beam. Such results agree with the experimental findings reported by other wood scientists indicating that knots located in the compression zone are less critical to the bending strength of beams (Wangaard 1950). In the case of vertical elliptic knots,

every 1 in. closer the knot center to the beam's upper rim will increase the stress concentration approximately 43%. However, such increase is not so pronounced in the case of horizontal knots.

## CONCLUSIONS

A mathematical model for predicting stress concentrations around knots of elliptic and circular shape in a simply supported laminated beam has been presented. Although the results reported involve only the case of two-layered laminated beams, the analysis can be modified to predict the stress concentrations in multi-layered laminated beams with many knots. Furthermore, the approach can be applied to the case of uniformly distributed load.

The decayed knots and knotholes will cause serious problems in stress concentration. However, if the knot is replaced by a wooden plug, stress concentration will be significantly reduced. It was found that surface curvature and knot dimension greatly influence the stress concentration. The horizontal elliptic knot has much higher stress concentration than those vertically oriented. When the knot is located at the high shear-moment ratio section (low bending moment area) in a tension zone, regardless of its size and orientation, stress concentration problems are very minor. In contrast, if the knot is located at the low shear-moment ratio section (high bending moment area), stress concentrations will be considerably higher and significant reduction in beam bending strength is expected.

## ACKNOWLEDGMENTS

The author wishes to thank Mr. C. C. Chen, graduate student in the Department of Forestry at Auburn University, for his assistance in the numerical calculations and data plotting. Also, the author would like to express his appreciation to Mr. D. Pugel for sharing his valuable research information on the elastic properties of knots.

## REFERENCES

BARTOLOMEO, E. D. 1980. A finite element investigation of the stress distribution around knots in wood. M.S. thesis, SUNY, Syracuse, NY.

FREAS, A. D. 1962. Factors affecting strength and design principles of glued laminated construction. USDA For. Prod. Lab. Res. Rep. 2016.

GOODMAN, J. R., A. DABHOLKER, AND J. BODIG. 1980. Verification of a model for tension behavior of wood with knots. Presented at the 34th FPRS Annual Meeting, Boston.

KOCH, P. 1972. Utilization of the southern pines. Vol. 1: The raw material. Agricultural Handbook No. 421.

LEKHNITSKII, S. G. 1969. Anisotropic plates, Translated by S. W. Tsai and T. Cheron, Gordon and Breach Science Publishers, New York, London.

PHILLIPS, G. E., J. BODIG, AND J. R. GOODMAN. 1981. Flow-grain analogy. Wood Sci. 14(2): 55–64.

PRICE, E. W. 1967. Stress distribution in the vicinity of knot-holes in construction lumber under bending forces. M.S. thesis, College of Forestry, University of Washington.

PUGEL, A. D. 1980. Evaluation of selected mechanical properties of coniferous knotwood. M.S. thesis, Department of Forest and Wood Sciences, Colorado State University.

SAVIN, G. N. 1961. Stress concentration around holes. Pergamon Press, London, New York, Paris.

SIIMES, F. E. 1944. Mitteilungen über die Untersuchung von Festigkeitseigenschaften der Finnischen Schnittwaren. Silvae Orbis. No. 15. Berlin-Wannsee.

SMITH, C. B. 1944. Effect of elliptic or circular holes on the stress concentration in plates of wood or plywood considered as orthotropic materials. USDA For. Prod. Lab. Res. Pre. No. 1510.

TANG, R. C. 1968. Boundary value problems in anisotropic elasticity. Ph.D dissertation, North Carolina State University, Raleigh, NC.

UENOYA, M., AND R. G. REDWOOD. 1978. Buckling of webs with openings. Computers and Structures 9(2):191–199.

USDA FOREST PRODUCTS LABORATORY. 1974. Wood handbook: Wood as an engineering material. USDA Agriculture Handbook No. 72, Rev.

WANGAARD, F. F. 1950. The mechanical properties of wood. John Wiley & Sons, Inc., New York.